Petri-Net based modelling and Multi-objective optimal deployment for WRSN

Huaiyu Qin*, **. Leijun Xu*.
Buhui Zhao*. Jun Wan***

*School of Electrical and Information Engineering, Jiangsu University, Zhenjiang 212000, P R China
China (Tel: 0086-511-88791240; e-mail: xlking@ujs.edu.cn, zhaobuhui@ujs.edu.cn)
** Jiangsu University of Science and Technology, Zhenjiang 212000, P R China
China (e-mail: qhy@just.edu.cn)
***Changzhou University, Changzhou 213000, P R China
China (e-mail: qiaosan@sina.com)

Abstract: Wireless Rechargeable Sensor Network (WRSN) is a very promising way to solve the energy unsustainability, which has attracted wide attention in academic circles. However, there is still a lack of an effective model to fully express WRSN, and the existing works focus on mobile charging or preset candidate locations, and little attention is paid to the deployment strategy of fixed chargers. To this end, the Generalized Synchronizing Colored Cyber Petri Nets is presented to establish the charging model in order to describe the system directly and comprehensively. Due to the conflicting objectives and the infinite deployment location, the Charger Deployment Optimization problem is difficult to be solved by traditional optimization method. Then, A Charger Deployment Multi-Objective Genetic Algorithm based on NSGA2 has been proposed. Simulation results show that the proposed algorithm can optimize both the charging power and the network utility, having a better performance than the algorithms of MOEA/D and SPEA2.

***Keywords**:* Wireless rechargeable sensor networks, Petri-nets, Charging deployment, Multi-objective optimization, Genetic algorithm.

1. INTRODUCTION

Traditional wireless sensor networks usually use batteries to charge nodes, which determines the limited life of the nodes. In addition, the cost of renewing the battery is particularly high. Energy harvesting arises at the historic moment, and wireless rechargeable sensor network is a typical example where the nodes can harvest RF radiation signals from the environment, known as wireless charging. It originates from the electric power transmission, transmitting the electric energy to the equipment wirelessly by electric magnetic resonance or electromagnetic radiation, thus realizing the convenient transmission of the energy.

For no dead angle coverage, large number of sensor nodes are usually deployed for outdoor scenarios such as earthquake warning, environmental monitoring, etc. However, the problem of power supply comes with it. Whether economical or feasible, it is not realistic to replace batteries artificially. Although mobile charging can accurately solve the problem of energy replenishment, it is vulnerable by natural conditions such as geology, meteorology and hydrology with a long delay, thus difficult to play its role. Fixed charger can fully cover the sensor nodes in the area and provide enough energy for them with lower maintenance cost. On the one hand, from the point of view of the sensor nodes, the more harvesting energy to be obtained, the better. On the other hand, considering the fixed charger deployment cost, it is desired to meet the energy requirements of the whole network with less transmission power. Nevertheless, the above objectives are in conflict with each other. Single optimization of one is bound to be at the expense of another goal.

The fixed charger deployment is similar with the coverage problem in traditional wireless sensor networks, but the existing solutions cannot be used directly in our research for the following two reasons. First, the direction of signal transmission is different. In our problem, the sensor node receives the RF signal from the charger, while the traditional coverage problem deploys the sensor node to sense the target states. Secondly, the wireless charging models are different from the coverage models in the traditional wireless sensor network which can be classified as physical coverage and probabilistic coverage. Physical model refers to specific deployment topology, and the target points in the region can be monitored by at least one sensor node. Probabilistic model utilizes probabilistic statistical methods to predict the possibility of target points being monitored. These two models are distinct from the wireless charging model.

From the above, the relation of number, position and power of the charger is closely linked, rather than isolated. It is hoped that maximum charging utility will be obtained with a minimum cost. However, in practice, the less the transmitting power, the smaller the network utility; conversely, the greater the network utility.

The contributions are summarized as follows.

1. It is the first time that Petri nets is used for the charger deployment Optimization, and a Generalized Synchronizing Colored Cyber Petri Nets is proposed, which can express the position and power transfer between charger and sensor nodes.

2. In 3D scenario, the Charger Deployment Optimization (CDO) is constructed as a joint optimization problem of network utility and charger transmitting power. And it has been proved to be NP-hard (NP-Hardness, non-deterministic polynomial-time hardness). A multi-objective optimization genetic algorithm is proposed to obtain the sub-optimal solution.

3. The proposed algorithm is evaluated by large-scale simulation, and the effects of charger number, node power consumption, node number and on deployment are studied.

The remainder of the paper is organized as follows. Section 2 reviews some related works on wireless charger deployment and the application of Petri nets. Section 3 constructs the charging model based on Petri nets. Section 4 proposes the charger deployment strategy. Section 5 evaluates the efficiency of the proposed algorithm. Section 6 concludes the paper.

2. REVIEW OF WRSN AND PETRI NETS

2.1 Wireless Rechargeable Sensor Network Review

Similar to the traditional network node deployment, the wireless charger deployment also encounters the coverage problem, but the difference is that the charging effect varies with the distance between the node and the charger. Therefore, traditional solution is difficult to provide guidance for wireless charger deployment.

In recent years, some scholars have studied the deployment of wireless chargers. He et al. divided the charger deployment into static and dynamic ones, which involved point provisioning and path provisioning respectively. They were deployed in the vertex of equilateral triangles, and the number of chargers was reduced as much as possible by expanding the triangular area. The proposed point provisioning has been proved to be able to achieve sub-optimal performance, while the path provisioning is actually close to the optimal performance (He et al., 2013). On the background of 3D beam directed antenna, Liao et al. proposed two greedy algorithms, namely, greedy cone selection algorithm (NB-GCS) based on nodes and greedy cone selection algorithm (PB-GCS) based on node pair, assuming that chargers are deployed in fixed height grids. The latter is superior to the former in the number of nodes, but the complexity of the former is lower (Liao et al., 2014). To optimize the deployment and quantity of chargers, Ejaz et al. used the trade-off coefficient to balance charging optimization and energy fairness (Ejaz et al., 2015). Jiang et al. considered charging path planning and mobile charger retention point jointly through path planning, candidate stopover point, so as to obtain the best charging efficiency of mobile charger (Jiang et al., 2017). Lin et al. developed the deployment strategy of the charger when the energy consumption of the nodes was not uniform (Lin, Li, & Chang, 2016). Nicolae et al. studied the utility of directional antennas and synchronization mechanism for prolonging the life of the sensor nodes from a ground deployed WSN. It was proved through simulation that the node's life is desired to reach several years (Nicolae, Popescu, Dobrescu, & Costea, 2016).

In order to ensure that the electromagnetic radiation intensity at any point in the charging area is less than a given threshold R_t, Dai et al. put forward a safe charging problem for charger scheduling(SCP), which maximizes the charging effectiveness within the safe threshold range of electromagnetic radiation. The gap between the maximum electromagnetic radiation point algorithm and the optimal algorithm is only 6.7, which is 34.6% better than the greedy algorithm (Dai et al., 2017). To adjust the transmitting power continuously, the optimization problem was transformed into the traditional linear programming, and the redundant constraints were removed, and a series of distributed algorithms were designed. Simulation results showed that the average performance of the overall charging utility is 41.1% better than the existing algorithms (Dai, Liu, et al., 2018). Then, Li et al. proposed a region segmentation algorithm to reduce the transmission power to a safe threshold, so that the lowest energy utility nodes were maximized (Li et al., 2019). Lai et al. sought the optimization goal of minimum charger position and shortest charging time. A two-step solution was proposed to minimize the number of charger positions and then allocate residence time according to charging requirements. Compared with the minimum group partition scheme, the number of charging positions and the total charging time can be saved by 60% (Lai & Hsiang, 2019). Sheikhi et al. put forward a solution for the combination of mobile charger and fixed charger. The fixed charging station uses grid elements to form a virtual area, and the charging stations coordinate with each other to guide the mobile chargers in the area (Sheikhi et al., 2019). Liu et al. studied the joint data acquisition and energy acquisition for mobile receiver in rechargeable wireless sensor networks. Long distance relay was proposed to select the sensor node which is close to each other, so as to assist the data transmission of the farther sensor node, synthesize the strategy of power allocation, relay selection and slot scheduling, and maximize the utility of the network (Liu, Lam, Han, & Chen, 2019). C. Lin et al. studied the cooperative charging decision problem in wireless rechargeable sensor networks. Based on the game theory, the mobile charger was regarded as the player, and the game cooperative charging scheduling strategy was designed to obtain the optimal Pareto solution (C. Lin et al., 2018). Yang et al. proposed a firefly algorithm based on adaptive attraction factor and dynamic position updating mechanism to deploy chargers. Simulation results showed that the IFA algorithm is superior to several reference algorithms for comparison in terms of accuracy and convergence speed (Yang et al., 2018).

2.2 Petri Nets Review

Due to the integration of mathematics and graphic representation, Petri nets have unique advantages in network modelling, especially in production scheduling, transportation network and so on. Li et al. built the production scheduling of flexible manufacturing system (FMS) by using time-delay petri nets, and obtained the optimal scheduling strategy by means of heuristic algorithm (Li, Wu, Feng, & Rong, 2015). Kadri et al. proposed a variable arc weight Petri net to solve the scheduling of shared bicycles, and used genetic algorithm to ensure that bicycles are available for pick up and vacant berths available for bicycle drop off at every station. Their research reflected the advantages of Petri net in modelling and performance analysis of complex dynamic systems (Kadri, Labadi, & Kacem, 2015). In (Ren et al., 2010), the operation sequences of jobs and the allocation of resources were modelled logically by a Petri net. In the proposed genetic algorithm, the operation sequence of all jobs in the system was encoded as a chromosome. By using the deadlock-avoidance Petri net controller for the system, the chromosome was tested and amended so that it could be decoded into a schedule that satisfies the resource constraint and the deadlock-free constraint. Thus, all chromosomes in the algorithm were corresponding to feasible schedules. Fang et al. presented a deadlock-free scheduling scheme and optimization for underground locomotive transportation system. The designed maximal marking boundary setting algorithm of deadlock-free schedule and genetic algorithm provided reliable theoretical foundation for locomotive transportation system dispatching (Fang et al., 2013). Cao et al. presented a genetic algorithm embedded search strategy over a hierarchical colored timed Petri net (HCTPN) for semiconductor wafer fabrication (Cao et al., 2010). Zhu et al. constructed a modular surface operation model based on the extended timed place Petri net (ETPPN) for the precision guidance of aircraft movement under the control of the advanced surface movement guidance and control system (A-SMGCS). Then, they presented algorithms for chromosome validation and amendment, crossover and mutation respectively (Zhu et al., 2013). Gonsalves et al. dealt with the performance modeling and the optimization of concurrent service systems, and demonstrated the effectiveness of the novel Client Server Petri net model editor–simulator–optimizer with the practical example of an automobile purchase concurrent service system (Gonsalves & Itoh, 2011). Wan et al. proposed a new approach for the modeling and VHDL implementation of digital systems based on an extended class of Petri nets and defined the generalized synchronous self-modifying net (GSSN) to describe digital systems. Based on a new kind of D flip-flop, known as multi-input and multi-clock D flip-flop, a specific conversion method from Petri nets models to VHDL codes was presented, providing a set of tools from specification level to implementation level to support complete services for modeling, analysis, simulation and implementation of digital systems (Wan et al., 2017). Song et al. used colored Petri nets to express and expand fault tree for reliability analysis of train system. This modeling approach can remove the limitation that the fault tree can only evaluate dynamic systems with event-repair operations and time-dependent properties, and can combine nonlinear relations such as feedback (Song & Schnieder, 2018). Wu et al. proposed a quantitative security analysis model via time-colored Petri nets (Wu & Zheng, 2018). G. Y. Zhang et al. implemented a multi-component collaborative design methodology for a liquid rocket engine and took Petri nets for performance driven design process based on extended Petri nets which can effectively couple existing knowledge resources, solve any conflict arising from different knowledge, and achieve an optimal strategy (G. Y. Zhang et al., 2017) . Jiang et al. used colored Petri net to construct a hierarchical distributed control system (DCSs) for automatic fault detection and recovery of power transmission system (PTSs), to prevent traditional transmission lines from fault interference (Jiang et al., 2018). Si et al. designed a general genetic algorithm (GGA) framework based on Petri nets, which can be used to optimize any given business process modeled by colored Petri nets, so as to intelligently optimize resource allocation in business processes (Si, Chan, Dumas, & Zhang, 2018). Lorena et al. proposed an extension and application of green procurement model based on colored Petri net to avoid the combination explosion of variables, which was suitable for the green procurement process of any organization (Lorena & Leonardo, 2018).

However, the role of Petri Nets in wireless rechargeable sensor network has not been reported yet.

3. PROBLEM FOMULATION

3.1 Charger Deployment Modelling

Assuming that there is a set of m static chargers $C = \{c_1, c_2, \cdots, c_m\}$ and n sensor nodes $S = \{s_1, s_2, \cdots, s_n\}$ in a three-dimensional space. The nodes can receive power from the chargers and thus maintain normal operation. In this paper, Friis's free space equation is used as the wireless charging model (He et al., 2013), namely,

$$P(d_{ij}) = \frac{G_S G_r \eta}{L_p} \left(\frac{\lambda}{4\pi(d_{ij}+\beta)}\right)^2 p_i \qquad (1)$$

where d_{ij} represents the Euclidean distance between charger i and node j, G_S is the source antenna gain, G_r is the receive antenna gain, λ is the wavelength, L_p is polarization loss, and η can be referred to as rectifier efficiency, β is a parameter to adjust the Friis' free space equation. Since all the above parameters are constants, (1) can be simplified to (2),

$$P(d_{ij}) = \frac{\tau}{(d_{ij}+\beta)^2} \qquad (2)$$

where $\tau = \frac{G_S G_r \eta}{L_p} \left(\frac{\lambda}{4\pi}\right)^2 p_i$, the coordinates of charger and sensor node are respectively $(x_i, y_i, z_i), (x_j, y_j, z_j)$, then $d_{ij}^2 = (x_j - x_i)^2 + (y_j - y_i)^2 + (z_j - z_i)^2$, p_i represents the transmitting power of i^{th} charger.

It can be seen that the greater the transmitting power and the smaller the distance from the charger, the more power a sensor node receives and vice versa. The power received varies with the location of the charger, so Charger Deployment Optimization (CDO) is fundamentally different from the traditional wireless sensor network coverage. It is expected that the charger will emit as little power as possible, while the network will be as effective as possible. Network utility can be defined as,

$$u(s_j) = \sum_{i=1}^{m} P(d_{ij}) \qquad (3)$$

With the aforementioned models, the Charger Deployment Optimization (CDO) can thus be described and mathematically formulated.

$$\begin{aligned} &\min \ \sum_{i=1}^{m} p_i, \max \ \sum_{j=1}^{n} u(s_j) \\ &s.t. \ \forall u \in \mathbb{R}^2, \quad l_j \le u(s_j) \end{aligned} \qquad (4)$$

The constraint condition indicates that the network utility cannot be less than the power consumption of the node, and l_j represents the consumption power of j^{th} node.

It is very challenging to solve the CDO from the above formulation. First, since the location of deployable chargers is infinite, in other words, there can be an infinite number of chargers, which makes it extremely difficult to analyze. Second, even if the number of chargers can be reduced, the power matching is still a knapsack problem, and the knapsack problem is NP hard.

3.2 Petri Nets Modelling

Generalized Synchronizing Colored Cyber Petri Nets (GSCCPN) is used for modelling, and the definition will be given below.

Definition 1 The condition that six-tuple $\sum(S, T; F, K, W, M_0)$ containing k colors constitutes GSCCPN is

(1) $\mathrm{N} = (S, T; F)$, named as a basic Petri net.

(2) K is the capacity function of N.

(3) W is weight function of N, representing a K-dimensional nonnegative vector assigned to each directed arc.

(4) M_0 is the initial marking.

Definition 2 M is the marking of N, $\mathrm{t} \in \mathrm{T}$

Supposing that the marking $M(s)$ contains 4 colors, and $M(s) = [x, y, z, p] = [M(s)_1, M(s)_2, M(s)_3, M(s)_4]$

(1) $\forall \mathrm{s} \in {}^{\cdot}t : M(s)_4 \ge W(s,t)_4 \wedge \forall \mathrm{s} \in t^{\cdot} : M(s)_4 + W(t,s)_4 \le K(s)_4$

If transition t is fired, it can be recorder as M [t > .

(2) If transition t is fired on *M*, *M* can be changed to be *M'*, and *M'* is given as follows.

$$M'(s) = \begin{cases} [M(s)_1, M(s)_2, M(s)_3, M(s) - W(s,t)] & s \in {}^{\bullet}t - t^{\bullet} \\ [M(s)_1, M(s)_2, M(s)_3, M(s) + W(t,s)] & s \in t^{\bullet} - {}^{\bullet}t \\ [M(s)_1, M(s)_2, M(s)_3, M(s) - W(s,t) + W(t,s)] & s \in {}^{\bullet}t \cap t^{\bullet} \\ M(s) & s \notin ({}^{\bullet}t \cap t^{\bullet}) \end{cases}$$

(5)

The relationship between *M* and *M'* is denoted by M [t > *M'*.

The state equation of GSCPN can be written as

$$M' = M_0 +\!\!\to C \cdot U \quad (6)$$

where the matrix operator $+\!\!\to$ represents the substitution plus, C is the incidence matrix, and U is the matrix representation of the sequence of concurrent steps $U_1 U_2 \cdots U_k$.

Hence, the state equation of GSCCPN can be written as

$$M(t_n) = M_0 + C \cdot \left[\int_{\tau_0}^{\tau_n} () \right] d\tau \quad (7)$$

Figure 1 shows a simple GSCCPN of charging model with two colors (red, green). The initial marking is $M_0 = ([x_1, y_1, z_1, p_1], [x_2, y_2, z_2, 0])$, and the first three components of the marking are represented in red, representing the position; the fourth green component represents power. The new marking after firing is $M_1 = ([x_1, y_1, z_1, p_1], [x_2, y_2, z_2, W(T_{12}, S_2)])$ by transition firing condition.

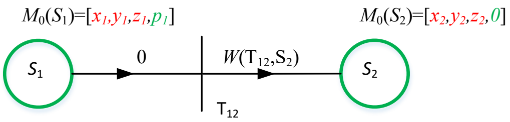

Fig. 1. Generalized Synchronizing Colored Cyber Petri Nets, GSCCPN.

The GSCCPN model of CDO is shown in Fig. 2, which indicates, transmitting power, consumption power, node position. The important symbols are shown in Table 1. Here, a place with two colors represents charger and sensor node, where the red markings indicate the 3D coordinates, while the green marking indicates the transmitting power or the received power of the node. From the above definition, $M(P_j)_4$ is the harvesting power of j^{th} sensor node, it can be written as

$$M(P_j)_4 = \sum_{i=1}^{m} W(T_{ij}, P_j)_4,$$
$$l_j = W(P_j, T_j), \quad u_j = K(P_j)_4,$$

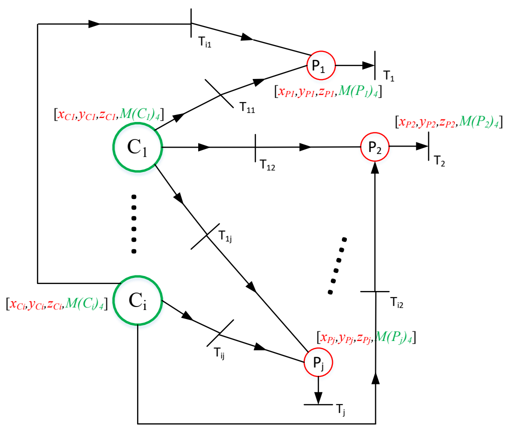

Fig. 2. GSCCPN model of Charger Deployment

Table 1. List notations

Notation	Definition
C_i	i^{th} Charger
P_j	j^{th} Sensor node
T_{ij}	The j^{th} Sensor node is charged by i^{th} Charger
T_j	The j^{th} Sensor node is consuming power

The GSCCPN dynamic equation of CDO can be expressed as

$$M(P_j)_4 = \left[\sum_{i=1}^{m} W(T_{ij}, P_j)_4 - W(P_j, T_j)_4\right] \cdot \left[\int_{\tau_0}^{\tau_n} () \right] d\tau \quad (8)$$

It can be seen that the following conditions must be satisfied in order to maintain sufficient energy of sensor nodes,

$\sum_{i=1}^{m} W(T_{ij}, P_j)_4 - W(P_j, T_j)_4 \geq 0$. Hence, the GSCCPN model of charger deployment is as follows:

$$\min \sum_{i=1}^{m} M(C_i)_4, \max \sum_{j=1}^{n} W(T_{ij}, P_j)_4$$
$$s.t. \quad W(P_j, T_j) \leq M(P_j)_4 \quad (9)$$

4. CHARGER DEPLOYMENT OPTIMIZATION

The two optimization objectives of Charger Deployment Optimization are conflict with each other, that is, the optimal solution cannot be achieved at the same time, hence it is necessary to make a trade-off between the two objectives. However, the problem is NP hard, and the traditional optimization method is difficult to solve. Therefore, A Charger Deployment Multi-Objective Optimization Genetic Algorithm (CDMOGA) based on NSGA2 is proposed. Assuming that all sensor nodes in the network can receive the power emitted by the chargers.

4.1 NSGA2 Algorithm

NSGA2 is one of the most popular algorithms. By means of fast non-dominate sorting algorithm, crowded competition selection method and elite strategy, the pareto optimal solution can be searched efficiently. This method guarantees the diversity of population and prevents individual loss. The principle of the standard NSGA2 algorithm is as follows.

Firstly, the initial population D_t was randomly generated and sorted according to different non-dominate hierarchies. A fitness value equal to the non-dominant level is assigned to each solution. Binary tournament selection, mutation and recombination operators are used to generate offspring population. Then the following steps is repeated until the number of iterations reach the maximum.

Step1. Combine the parents and offspring populations, and create $P_t = D_t \cup E_t$. According to algorithm 1, perform fast non-dominant sorting in P_t and identify different frontiers Fr_i.

Step2. Set a new population $D_{t+1} = \emptyset$, and let $counter\ i = 1$. $While\ |D_{t+1}| + |Fr_i| < N, do\ D_{t+1} = D_{t+1} \cup Fr_i\ and\ i = i + 1$.

Step3. Choose (N-$|D_{t+1}|$) most general solution from binary crowding tournament selection operator, and insert them into D_{t+1}.

Step4. Create offspring E_{t+1} from by D_{t+1} binary crowding tournament selection, crossover and mutation operators, and let $t = t + 1$.

Fast non-dominate sorting algorithm
Input: population P
Output: The non-dominated fronts $(Fr_1, Fr_2, \cdots)$

```
For each p ∈ P
    For each q ∈ P
        If (p < q) then
            S_p = S_p ∪ {q}
        else if (q < p) then
            n_p = n_p + 1
        If n_p = 0 then
            F_1 = F_1 ∪ {p}
i = 1
while F_i <> ∅
    H = ∅
    For each p ∈ Fr_i
        For each q ∈ S_p
            n_q = n_q − 1
            If n_q = 0 then H = H ∪ {q}
i = i + 1
Fr_i = H
```

Algorithm1: The pseudocode of fast non-dominate sorting algorithm

The non-dominant sorting process and the steps to fill the population D_{t+1} can be performed together. The crowd ordering of solutions in frontier Fr_i is performed by crowding distance, while Fr_i is the last frontier which cannot be fully accommodated.

The crowding comparing operator compares two solutions and returns the victor. The choice is based on the following two points: non-dominate ranking r_i and the local crowding distance within the population. The crowding distance of solution *i* is the measurement of the search space around *i*, which is not occupied by any other solution in the population. Based on r_i and d_i, the binary crowding tournament selection operator works as follows.

Solution i beats solution j in the race if the following conditions are true.

(1) If $r_i < r_j$ (This condition ensures that the selected solution lies in a more non-dominat position).

(2) If $r_i < r_j$ and $d_i < d_j$ (When both solutions are on the same front and the above conditions cannot be applied, the method is applied; in this case, the solution in a less crowded area wins).

4.2 Dynamic crowding distance Algorithm

The horizontal diversity of the pareto frontier is very important in multi-objective optimization, which is achieved by eliminating the redundant individuals in the dominance concentration. To remove redundant individuals, NSGA2 uses crowding distance measurement. The removed individuals with lower crowding distance values have a higher priority. The crowding distance value is calculated by the following formula,

$$CD_i = \frac{1}{N_{obj}} \sum_{z=1}^{N_{obj}} |F_{i+1}^z - F_{i-1}^z| \tag{10}$$

Here, N_{obj} is the number of objectives, F_{i+1}^z is z^{th} objective of *i+1* individual, F_{i-1}^z is the z^{th} target of the $(i-1)^{th}$ individual after sorting the population according to the crowding distance value. The main defect of crowded distance is lack of uniform diversity in obtaining non-dominated solutions. To solve this problem, (Luo et al., 2018) proposed a dynamic crowding distance algorithm. The dynamic crowding distance of individuals is:

$$DCD_i = \frac{CD_i}{\log(1/Var_i)} \tag{11}$$

CD_i can be obtained by (10), and Var_i can be obtained by (12),

$$Var_i = \frac{1}{N_{obj}} \sum_{z=1}^{N_{obj}} (|F_{i+1}^z - F_{i-1}^z| - CD_i)^2 \tag{12}$$

Var_i is the variance of the crowded distance between the *ith* neighbouring individuals.

4.3 Genetic representation of the algorithm

In the traditional genetic algorithm, chromosomes are represented by binary strings. In order to calculate the value of the objective function, the binary strings (genotypes) need to be converted to the real number space (phenotypes), which will inevitably increase the calculation cost. Therefore, a more effective real number representation method is adopted in this paper, which is a direct coding mechanism, and the genotype and phenotype are exactly the same. Each charger gene is represented by a four-digit vector, the first of which represents the transmitting power of the charger, and the last three represent the three coordinates of the charger, as shown in figure 3.

Charger1	Charger 2		Charger N
Transmitting power1 &Coordinates 1	Transmitting power 2 &Coordinates 2	……	Transmitting power N &Coordinates N
Gene1	Gene 2		Gene N

Fig. 3. Genetic representation of the algorithm.

4.4 Charger Deployment Multi-Objective Genetic Algorithm

First, an initial population of size M is generated. G chargers are uniformly distributed randomly, and the transmitting power is assigned to each charger. The power received by each sensor node is calculated through (1), and the objective function is calculated under the constraints mentioned above. Then offspring are created from existing populations through crowded race selection, crossover, and mutation operators.

A two-point crossover operator is designed, and the crossover point can be randomly selected between variables. The crossover rule is:

(1) Select the first m vectors from the first parent chromosome;

(2) choose the vector between m+1 and n from the second parent;

(3) choose the vector after the *nth* from the first parent chromosome;

Charger Deployment Multi-Objective Genetic Algorithm (CDMOGA)
Input: Network parameters
Output: Non-dominate solution
Step 1. Choose population of size M, crossover probability (P_C)and mutation probability (P_M), maximum iterations (gen_{max}), Set the iteration count from t=0;
Step 2. Generate initial population D_t according to the rules below
For $i = 1, \cdots, \mathrm{M}$ do
 Step 2.1. Generate G chargers randomly
 Step 2.2. Assign transmitting power and coordinate position for each charger;
Step 3. Evaluate each solution of the initial population according to the objective function and constraints;
Step 4. Create offspring population E_t by crowding tournament selecting, crossover and mutation in D_t;
Step 5. Let $P_t = D_t \cup E_t$;
Step 6. Perform fast non-dominate sorting for P_t, and generate non-dominate frontiers $Fr_1, Fr_2, \cdots$;
Step 7. Set $D_t + 1 = \emptyset$; $i = 1$;
 While $|D_{t+1}| + |Fr_i| < M$ do
 $(D_{t+1} = D_{t+1} \cup Fr_i, i = i + 1)$;
 If $|D_{t+1}| < M$ then
 Calculate DCD in Fr_i, and arrange them in descending order, Add the first solution $M - |D_{t+1}|$ to D_{t+1} from Fr_i;
 If $t < gen_{max}$ then set $t = t + 1$, and return to Step 3.

These operators then combine genes to form a new progeny. For example, p1 and p2 are the parent chromosomes,

p1 = [a b c d e f g h],
p2 = [1 2 3 4 5 6 7 8],

If the intersection is between the third and sixth positions, then the offspring chromosome is:

child = [a b c 4 5 6 g h],

Some genes will be randomly selected for mutation after crossover, which can introduce features not belonging to the original population and prevent the algorithm from too fast convergence. Mutation operators usually select a pair of genes on the chromosome and flip their positions. A sliding mutation operator is developed in this paper, as shown in figure 4. Let x_{min} and x_{max} represent the minimum and maximum value of genes, and x is the current gene value. Slide direction is selected randomly, right or left, and the slide momentum is generated arbitrarily within the allowed range. However, the gene mutated by sliding cannot cross the boundary. Thus, the boundary conditions of the decision variables remain unchanged. In other words, lethal genes are always avoided.

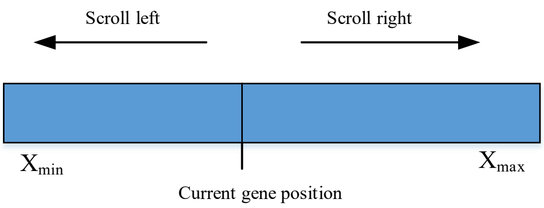

Fig. 4. Mutation Operator.

The offspring population is combined with the parent population. Then, a fast non-dominate sorting algorithm is applied to the combined population to identify different frontiers Fr_i $i = 1,2,\cdots$. And the new population contains the solutions of different non-dominant fronts step by step.

A new population of size M may not be able to accommodate all the frontiers of a combined population of size 2M. Therefore, if all solutions of the existing frontier cannot be accommodated by the new population, the dynamic crowding distance in the new population will be calculated. Then the solution is sorted in descending order according to the dynamic crowding distance value, and the solution required by the new population will be selected from the first one at the frontier. The above process continues until the maximum iterations is reached. Algorithm 2 shows the pseudocode of CDMOGA.

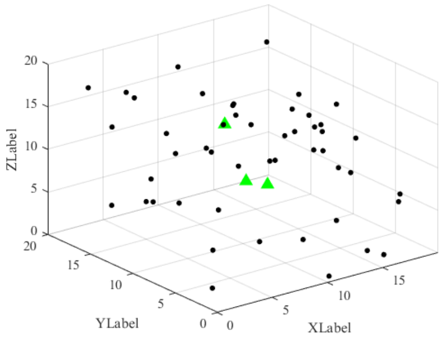

(a)

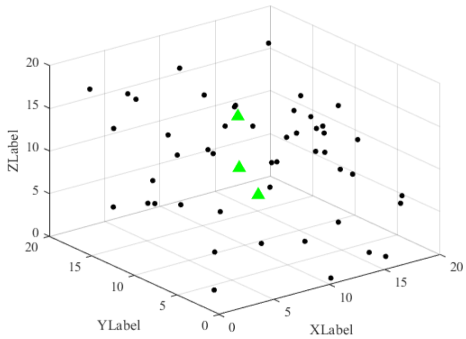

(b)

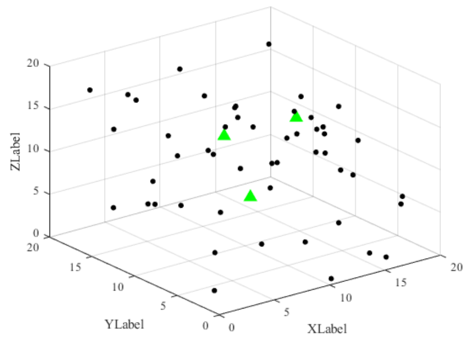

(c)

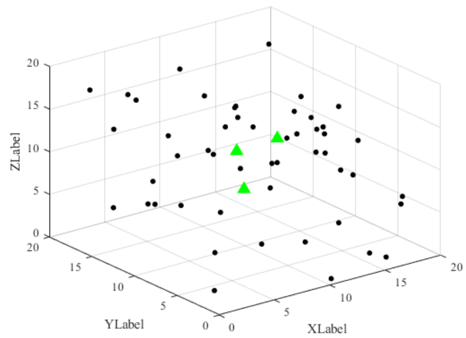

(d)

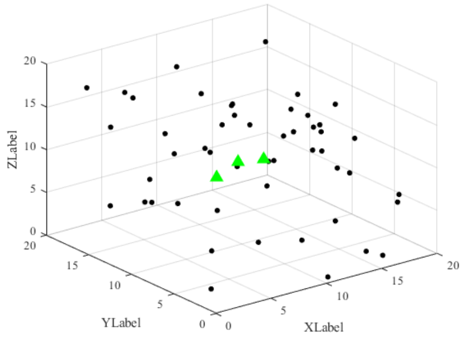

(e)

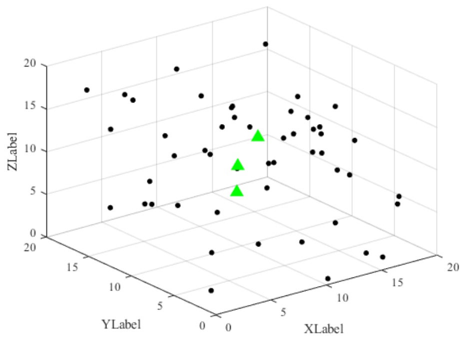

(f)

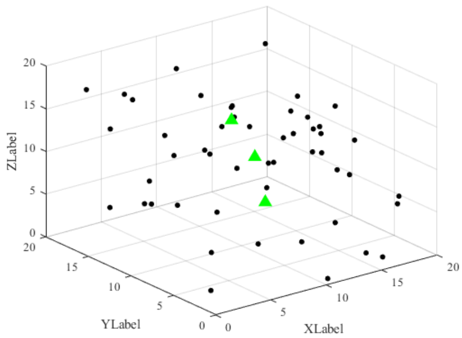

(g)

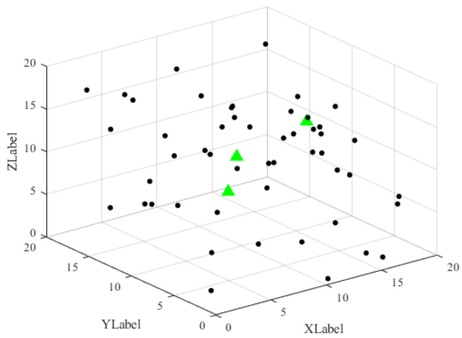

(h)

Fig. 5. 3 chargers deployment scheme of 50 nodes. (a)~(h) corresponds to scheme 1-8, respectively.

5. SIMULATION AND ANALYSIS

In this section, large scale simulation is conducted by MATLAB 9.0 and the algorithm performance will be evaluated.

5.1 Simulation settings

The experiment is carried out in a solid space with a side length of 20 meters. It is assumed that all sensor nodes in the space can receive the energy emitted by the charger, and the energy reception is additive for different chargers. Moreover, each point on the simulation curve represents the average of 50 simulation results. $G_S = 8\,dBi$, $G_r = 2\,dBi$, $\lambda = 0.33$, $\eta = 0.125$, $L_p = 0.5$, $\beta = 0.125$. Other parameters are shown in Table 2.

Table 2. Simulation parameters

Parameters	Description
WRSN cuboid	$20\text{м}(L) \times 20\text{м}(W) \times 20\text{м}(H)$
Number of sensor nodes	10，20，30，40，50
Number of Chargers	1,2,3,4,5,6,7,8
Node Distribution	Uniform Distribution
Average consumption power	50μw

5.2 Results

Figure 5 shows eight schemes for the deployment of 3 chargers under the random distribution of 50 sensor nodes, where the sensor node is represented by black solid dots and the green triangle represents the charger.

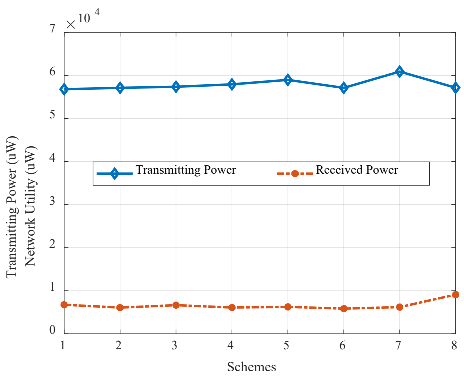

Fig. 6. Transmitting power and Received power of 8 schemes.

As can be seen from figure 6, the deployment position of the charger is slightly different, and the transmission power is not the same, but the total transmission power of the eight schemes is basically the same. Furthermore, the charger is basically deployed in the same area. This shows that although this algorithm can only obtain an optimal solution set, rather than a single optimal solution, the difference between different solutions is very small, which can effectively solve the charger deployment problem.

5.3 Performance comparison

CDMOGA is compared with MOEA/D (Q. F. Zhang & Li, 2007), SPEA2 (Zitzler & Thiele, 1999), and the following metrics for evaluation is considered:

(1) influence on receiving power and transmitting power with different nodes;
(2) influence on transmitting power with different power consumption;
(3) influence on transmitting power with heterogeneous nodes;
(4) influence on receiving power and transmitting power with different chargers.

Experiment 1. When the number of sensor nodes increases from 10 to 50, the receiving power and the transmission power are shown in figure 7 and figure 8, respectively. As can be seen in figure 7, the total received power is increased with the number of nodes, since in the case of a constant number of chargers and transmission power, the sensor nodes become more, i.e., the charged device is increased, so that the power received by the network is also increased. Figure. 8 shows the trend of transmission power changing with the number of sensor nodes. In general, the more sensors there are, the greater the transmission power is required. The reason is that the probability of the sensor nodes distributed to the region's edge is positively correlated with their own number. In addition, the transmission power of CDMOGA is 6% and 7.8% lower than that of MOEA/D and SPEA2, respectively, and the receiving power is 17.6% and 25.2% higher than that of latter. This is due to the fact that CDMOGA is more inclined to the elite strategy in the deployment strategy, so that the charger has lower transmission power and sensor nodes can receive higher power.

Experiment 2. The experiment simulates the trend of transmission power when the power consumption of sensor nodes increases from 50 to 250. As shown in Figure 9, the transmission power of the CDMOGA is increased from 57 mW to 285 mW, and the transmission power generated by MOEA/D and SPEA2 is increased from 62 mW, 63 mW to 310 mW, 330 mW, respectively, which reflects that the transmission power tends to increase with node power consumption, but the other two algorithms are 9.3% and 14.3% higher than CDMOGA, respectively. Therefore, the performance advantage of CDMOGA is more obvious as the node power consumption increases.

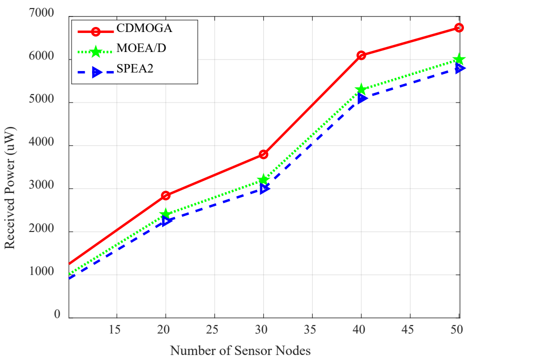

Fig. 7. Received power with the different sensor nodes.

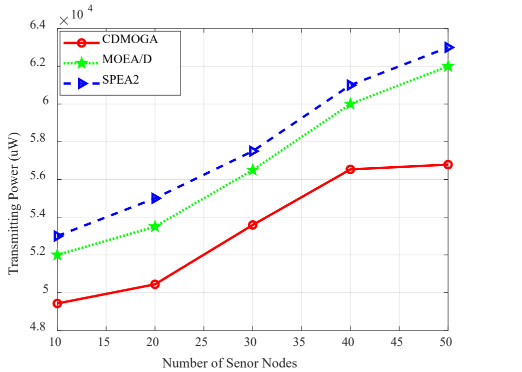

Fig. 8. Transmitting power with the different sensor nodes.

Experiment 3. In this experiment, the distribution position and number of the sensor nodes are unchanged, and the power consumption of the 10 nodes is increased to 100μW, as shown by the black square in Figure 10, and the power consumption of the remaining nodes is maintained at 50μW. The green triangle and the red pentagram represent the charger deployment position before and after the power consumption change, respectively. Since seven nodes with larger power consumption are on the right side of the region, two chargers are obviously moved to the right. At the same time, there are still 3 power-consuming nodes on the left side of the region, hence one charger remains in the original deployment area to ensure that the remaining left-hand nodes are not affected. Moreover, after the node power consumption changes, the transmitting power of the charger increases from 57mW to 100mW, almost doubled. It can be seen that even if the power consumption of a small number of nodes increases, the transmission power will increase significantly due to the superposition effect of position.

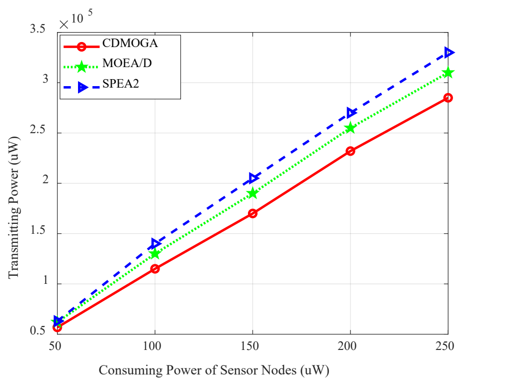

Fig. 9. Transmitting power with the different node power consumption.

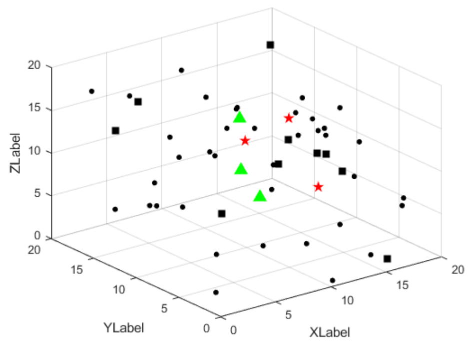

Fig. 10. Charger deployment with heterogeneous nodes

Experiment 4. The experiment evaluates the influence of the number of chargers on the transmission power. As shown in figure 11, the number of chargers increases from 1 to 8. When a single charger is deployed, its transmission power increases slightly because it is difficult to take into account all sensor nodes, but there is no significant change in the transmission power and reception power in the rest cases. The experimental results show that there is no obvious relationship between the number of chargers and the total transmission power. As long as the threshold of transmission power of a single charger is not exceeded, the number of chargers can be reduced as much as possible in order to reduce the deployment difficulty and maintenance cost.

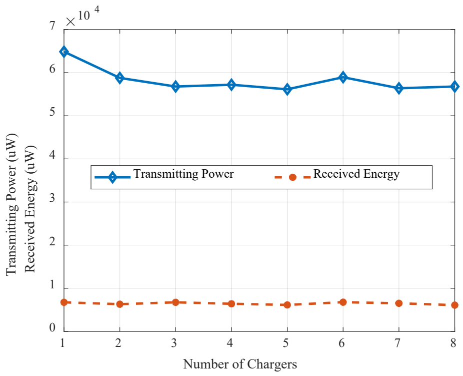

Fig. 11. Charger deployment with heterogeneous nodes

6. CONCLUSIONS

The paper innovatively proposes a generalized synchronizing colored cyber Petri net (GSCCPN) to model the charger deployment problem, and expresses the position, transmission and receiving power of network components concisely. For the first time, the optimization problem of charger deployment without presetting the candidate position of charger in three-dimensional space is formulated. The two objectives of the problem, that is, the transmitting power of the charger and the received power of the sensor node, are in conflict with each other, and optimizing one is bound to weaken the other. Therefore, the paper propose Charger Deployment Multi-Objective Optimization Genetic Algorithm (CDMOGA) based on NSGA2. First, CDMOGA uses the fast nondominant sorting algorithm to divide the feasible solution into several levels according to the priority. Secondly, CDMOGA remove the redundant individuals in the non-dominant set by the dynamic crowding distance algorithm, and then obtain the optimal solution set by gene crossing, mutation. Numerical simulation verifies the rationality and feasibility of the algorithm.

Due to the condition of homogeneous and heterogeneous nodes, and none of preset deployment position for the charger, our scheme can be well applied to the realistic system. In future work, the authors are interested to other practical situations such as charging radiation barriers.

ACKNOWLEDGMENTS

This work was supported by National Natural Science Foundation of China under Grant [NO. 61070058].

REFERENCES

Dai, H. P., Liu, Y. H., Chen, G. H., Wu, X. B., He, T., Liu, A. X., & Ma, H. Z. (2017). Safe Charging for Wireless Power Transfer. *Ieee-Acm Transactions on Networking*, 25(6), 3531-3544.

Dai, H. P., Liu, Y. H., Chen, G. H., Wu, X. B., He, T., Liu, A. X., & Zhao, Y. (2018). SCAPE: Safe Charging With Adjustable Power. *Ieee-Acm Transactions on Networking*, 26(1), 520-533.

Ejaz, W., Kandeepan, S., & Anpalagan, A. (2015, Aug. 30 2015-Sept. 2 2015). Optimal placement and number of energy transmitters in wireless sensor networks for RF energy transfer. Paper presented at the Personal, Indoor, and Mobile Radio Communications (PIMRC), *2015 IEEE 26th Annual International Symposium on*.

Gonsalves, T., & Itoh, K. (2011). GA optimization of Petri net-modeled concurrent service systems. *Applied Soft Computing, 11*(5), 3929-3937.

He, S., Chen, J., Jiang, F., Yau, D. K. Y., Xing, G., & Sun, Y. (2013). Energy Provisioning in Wireless Rechargeable Sensor Networks. *Ieee Transactions on Mobile Computing*, 12(10), 1931-1942.

Huan fang, Yang Lu, Zijun Xu, & Juan Yang. (2013). Resource allocation model and deadlock-free optimization scheduling for underground locomotive transportation. *Systems Engineering-Theory & Practice(08), 2087-2096*

Jiang, G. Y., Lam, S. K., Sun, Y. D., Tu, L. J., & Wu, J. G. (2017). Joint Charging Tour Planning and Depot Positioning for Wireless Sensor Networks Using Mobile Chargers. *Ieee-Acm Transactions on Networking*, 25(4), 2250-2266.

Jiang, Z. Y., et al. (2018). "Automatic Supervisory Control for the Self-Healing of Smart Grids Based on Colored Petri Nets." *Ieee Transactions on Electrical and Electronic Engineering* 13(11): 1612-1623.

Jun Wan, Buhui Zhao, & Huaiyu Qin. (2017). Petri net modeling and VHDL implementation of digital systems. *Application Research of Computers* (02), 458-462.

Kadri, A. A., Labadi, K., & Kacem, I. (2015). An integrated Petri net and GA-based approach for performance optimisation of bicycle sharing systems. *European Journal of Industrial Engineering*, 9(5), 638-663.

Lai, W. Y., & Hsiang, T. R. (2019). Wireless Charging Deployment in Sensor Networks. *Sensors*, 19(1), 19.

Lei Ren, Feng Wang, & Keyi Xing. (2010) . A Petri-net-based deadlock-free genetic scheduling for flexible manufacturing systems. *Control Theory & Applications* (01), 13-18

Li, L. L., Dai, H. P., Chen, G. H., Zheng, J. Q., Dou, W. C., & Wu, X. B. (2019). Radiation Constrained Fair Charging for Wireless Power Transfer. *Acm Transactions on Sensor Networks*, 15(2), 33.

Li, C., Wu, W. M., Feng, Y. P., & Rong, G. (2015). Scheduling FMS problems with heuristic search function and transition-timed Petri nets. *Journal of Intelligent Manufacturing*, 26(5), 933-944.

Liao, J.-H., Jiang, J.-R., & Ieee. (2014). Wireless Charger Deployment Optimization for Wireless Rechargeable Sensor Networks. *2014 7th International Conference on Ubi-Media Computing and Workshops (Umedia)*, 160-164.

Lin, C., Wei, S., Deng, J., Obaidat, M. S., Song, H. B., Wang, L., & Wu, G. W. (2018).

GTCCS: A Game Theoretical Collaborative Charging Scheduling for On-Demand Charging Architecture. *Ieee Transactions on Vehicular Technology*, 67(12), 12124-12136.

Lin, T. L., Li, S. L., & Chang, H. Y. (2016). A Power Balance Aware Wireless Charger Deployment Method for Complete Coverage in Wireless Rechargeable Sensor Networks. *Energies, 9*(9), 13.

Liu, Y., Lam, K. Y., Han, S., & Chen, Q. C. (2019). Mobile data gathering and energy harvesting in rechargeable wireless sensor networks. *Information Sciences*, 482, 189-209.

Lorena, C. M. and R. U. Leonardo (2018). "Sustainable procurement with Coloured Petri Nets. Application and extension of the proposed model." *Expert Systems with Applications,* 114: 467-478.

Nicolae, M., et al. (2016). "Scheduling Mechanism for Energy-Efficient Communication in Hybrid Wireless Sensor Networks." *Control Engineering and Applied Informatics,* 18(2): 95-102.

Sheikhi, M., Kashi, S. S., & Samaee, Z. (2019). Energy provisioning in wireless rechargeable sensor networks with limited knowledge. *Wireless Networks*, 25(6), 3531-3544.

Si, Y. W., et al. (2018). "A Petri Nets based Generic Genetic Algorithm framework for resource optimization in business processes." *Simulation Modelling Practice and Theory* 86: 72-101.

Song, H. F. and E. Schnieder (2018). "Evaluating Fault Tree by means of Colored Petri nets to analyze the railway system dependability." *Safety Science*, 110: 313-323.

Wu, D. H. and W. Zheng (2018). "Formal model-based quantitative safety analysis using timed Coloured Petri Nets." *Reliability Engineering & System Safety*, 176: 62-79.

Xinping Zhu, Xinmin Tang, & Songchen Han. (2013). Aircraft Initial Taxiing Route Planning Based on Petri Net and Genetic Algorithm. *JOURNAL OF SOUTHWEST JIAOTONG UNIVERSITY* (03), 565-573.

Yang, M., Wang, A. M., Sun, G., & Zhang, Y. (2018). Deploying charging nodes in wireless rechargeable sensor networks based on improved firefly algorithm. *Computers & Electrical Engineering*, 72, 719-731.

Zhang, Q. F., & Li, H. (2007). MOEA/D: A multiobjective evolutionary algorithm based on decomposition. *Ieee Transactions on Evolutionary Computation*, 11(6), 712-731.

Zhang, G. Y., Zhao, W. G., & Yan, X. T. (2017). Collaborative Design Implementation on the PN-PDDP Model for the Complex Coupled Rotor Systems. *Control Engineering and Applied Informatics*, 19(3), 69-78.

Zhengcai Cao, Hongxia Yu, & Fei Qiao. (2010). Petri-Net and GA-Based Approach to Modeling and Optimize for Semiconductor Wafer Fabrication. *ACTA ELECTRONICA SINICA* (02),340-344.

Zitzler, E., & Thiele, L. (1999). Multiobjective evolutionary algorithms: A comparative case study and the Strength Pareto approach. *Ieee Transactions on Evolutionary Computation*, 3(4), 257-271.